Inorganic Chemistry

Article

pubs.acs.org/IC

Four Polyanionic Compounds in the K–Au–Ga System: A Case Study in Exploratory Synthesis and of the Art of Structural Analysis

Volodymyr Smetana, John D. Corbett,* and Gordon J. Miller*

Ames Laboratory–DOE and Department of Chemistry, Iowa State University, Ames, Iowa 50011, United States

Supporting Information

ABSTRACT: The K–Au–Ga system has been investigated at 350 °C for <50 at. % K. The potassium gold gallides $K_{0.55}Au_2Ga_2$, KAu_3Ga_2, KAu_2Ga_4 and the solid solution KAu_xGa_{3-x} (x = 0–0.33) were synthesized directly from the elements via typical high-temperature reactions, and their crystal structures were determined by single crystal X-ray diffraction: $K_{0.55}Au_2Ga_2$ (**I**, *I*4/*mcm*, a = 8.860(3) Å, c = 4.834(2) Å, Z = 4), KAu_3Ga_2 (**II**, *Cmcm*, a = 11.078(2) Å, b = 8.486(2) Å, c = 5.569(1) Å, Z = 4), KAu_2Ga_4 (**III**, *Immm*, a = 4.4070(9) Å, b = 7.339(1) Å, c = 8.664(2) Å, Z = 2), $KAu_{0.33}Ga_{2.67}$ (**IV**, *I*-4*m*2, a = 6.0900(9) Å, c = 15.450(3) Å, Z = 6). The first two compounds contain different kinds of tunnels built of puckered six- (**II**) or eight-membered (**I**) ordered Au/Ga rings with completely different cation placements: uniaxial in **I** and **III** but in novel 2D-zigzag chains in **II**. **III** contains only infinite chains of a potassium-centered 20-vertex polyhedron ($K@Au_8Ga_{12}$) built of ordered 6–8–6 planar Au/Ga rings. The main structural feature of **IV** is dodecahedral $(Au/Ga)_8$ clusters. Tight-binding electronic structure calculations by linear muffin-tin-orbital methods were performed for idealized models of **I**, **II**, and **III** to gain insights into their structure–bonding relationships. Density of states curves reveal metallic character for all compounds, and the overall crystal orbital Hamilton populations are dominated by polar covalent Au–Ga bonds. The relativistic effects of gold lead to formation of bonds of greater population with most post-transition elements or to itself, and these appear to be responsible for a variety of compounds, as in the K–Au–Ga system.

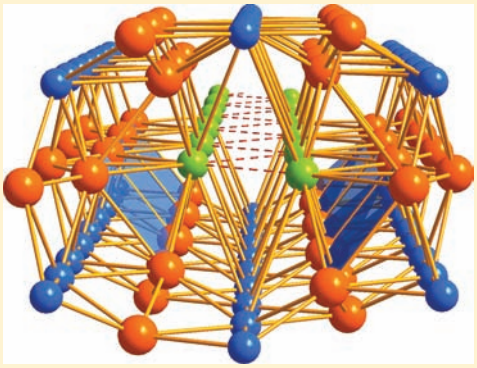

INTRODUCTION

The polyanionic chemistry of the triel elements Al–Tl continues to provide novel structures and interesting bonding features. Previous investigations of binary alkali metal–triel (A–Tr) systems, mostly with In and Tl, have resulted in the discovery of many new, polar intermetallic compounds,[1,2] and the addition of a third element into these systems has proved to be a good means for further development of this class of compounds. These additional atoms can play different roles in the formation of new compounds, depending in part on relative electronegativities and atom sizes or valence electron counts.

A large number of A–T–Tr compounds adopting novel structures have been discovered during the last 10 years when this third element is a late transition metal (T), mainly with Tr = Ga–Tl; for example, K_3Au_5Tl,[3] Rb_2Au_3Tl,[3] Na_4AuTl,[4] $Na_{10}NiGa_{10}$,[5] Na_3AgIn_2,[6] $Na_{13}(Cd_xTl_{1-x})_{27}$,[7] $Na_{35}Cd_{24}Ga_{56}$,[8] and $Na_{36}Ag_7Ga_{73}$.[9] Normally, the transition element and triel together create a formally anionic network, with the active metals A filling large coordination polyhedra. On the other hand, compounds with Li and Mg can be assigned into a separate class because both of these elements may occur either among the formal cations or in the anionic network, as in $K_{34}Mg_{13.9}In_{91.05}$[10] and $K_{34}Li_{12.70}In_{92.30}$.[11] It should be emphasized that the most productive third element in all of these investigations has been gold, evidently because of substantial relativistic effects in its bonding. These afford an enhanced (Mullikan) electronegativity for gold,[12] increased participation of the $5d^{10}$ shell in Au bonding, and larger Hamilton bond indices, especially for heteroatomic (polar) bonds.[2,3,13–15] For example, previous investigations of A–Au–In systems have resulted in several novel compounds with unique structural and bonding features; namely, K_3Au_5In,[3] AAu_4In_6, $K_{1.76}Au_6In_4$, $K_{0.63}Au_2In_2$,[13] KAu_4In_2,[16] $Na_2Au_6In_5$,[17] $Na_8Au_{11}In_6$,[18] $NaAuIn_2$,[19] and Na_3AuIn_2.[6]

Extending this chemistry systematically into A–Au–Ga systems has led to the discovery of several new compounds and an enhanced knowledge of the chemical behavior of these ternary systems. Some occasional investigations in A–Au–Ga systems for specific synthetic targets have resulted in only the novel $Na_{128}Au_{81}Ga_{275}$,[20] K_4Au_8Ga,[21] and $RbAu_xGa_{3-x}$,[22] indicating a new promising field for exploration. Herein, we report the synthesis and structural characterization of four new intermetallic compounds in the K–Au–Ga system: $K_{0.55}Au_2Ga_2$ (**I**), KAu_3Ga_2 (**II**), KAu_2Ga_4 (**III**), and $KAu_{0.33}Ga_{2.67}$ (**IV**). Some compounds with general compositions $\sim A_{0.5}T_2Si_2$ (A = Na, K; T = Pd, Pt) and disordered as well as fractional cation positions[23] are evidently isostructural and isoelectronic with **I**, but they have not been well refined. **II** is isostructural with the 12-electron $LaAl_3Ni_2$[24] and $BaZn_5$[25,26] but with two fewer

Received: September 14, 2011
Published: January 19, 2012

   dx.doi.org/10.1021/ic201999u | *Inorg. Chem.* 2012, 51, 1695–1702

electrons per formula unit (f.u.) and a distinctive bonding pattern. **IV** is isostructural with $RbAu_xGa_{3-x}$ for $x = 0.33$,[22] whereas **III** represents a new structure type.

EXPERIMENTAL SECTION

Synthesis. All materials were handled in a N_2-filled glovebox (≤0.1 ppm H_2O per volume). All compounds were obtained via standard high-temperature reactions of gold (99.995%, Ames Lab), gallium (99.99%, Alfa Aesar), and potassium (99.9%, Alfa Aesar). Weighed amounts of the elements were enclosed in tantalum tubes, which were crimped, welded, and then sealed into evacuated fused silica ampules to protect them from air, as described previously.[27] The reactions were prereacted at 500 °C for 24–48 h, cooled to 350 at 10 °C/h, annealed for 5–7 d, and cooled to room temperature by switching off the furnace. The synthetic conditions were chosen similar to those used earlier for A–Au–In systems.[13] Single crystals of **I**, **II**, and **III** were obtained from attempts to prepare compounds isostructural with $K_{0.63}Au_2In_2$, $K_{1.76}Au_6In_4$, and KAu_4In_6, respectively, whereas **IV** emerged during exploratory syntheses in the Au-poorer part of the ternary system. Existence of the only hitherto reported ternary K_4Au_8Ga[21] was also confirmed, but no other compound was found in the Au-rich part with <40% K (Figure 1). Single phase **II** and **III** were

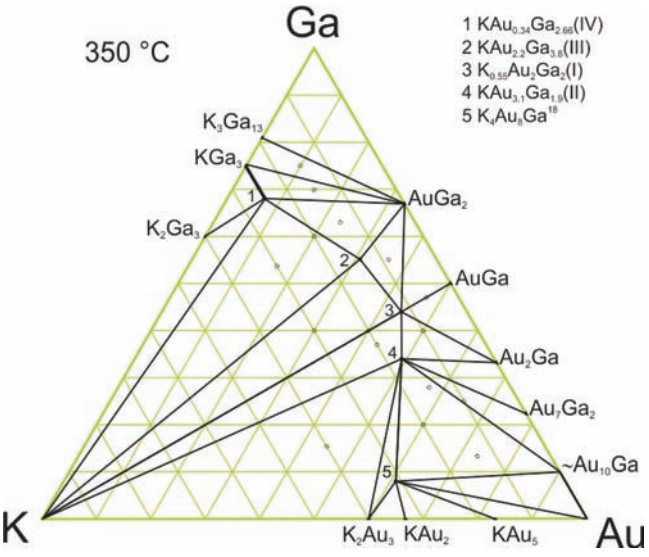

Figure 1. K–Au–Ga phase diagram at 350 °C. Small open circles identify compositions loaded; positions labeled 1–5 mark the phases identified by single crystal X-ray diffraction. A complete listing of products for each composition loaded is in Table S1 of the Supporting Information.

synthesized according to X-ray powder diffraction after determination of the correct composition from single crystal refinements, whereas **I** was evidently obtained pure from the initial reaction because the excess of K was not detected by X-ray powder diffraction analysis, a common event. A sample of "$K_{0.25}Au_2Ga_2$" was also prepared under the same conditions to check for any homogeneity region in **I**. Shifts of the unit cell parameters were not statistically significant, and the product was found to contain both $K_{0.55}Au_2Ga_2$ and AuGa. In contrast, a homogeneity range was discovered around composition **IV**, with the title compound representing the Au saturation point. All compounds have metallic lusters and are stable against prolonged exposure to air and water at room temperature (no changes were observed by eye or by powder X-ray analysis after 2 months). Thin, protective surface layers of elemental gold may again pertain.[13]

X-ray Diffraction Studies. Powder diffraction data were collected at room temperature with the aid of a Huber 670 Guinier powder camera equipped with an area detector and Cu K_α radiation (λ = 1.540 59 Å). The samples were dispersed on Mylar sheets with the help of vacuum grease and fixed using two split Al rings. The lattice parameters were refined using the WinXPow program.[28] Single crystals obtained from the reactions were fixed on glass fibers. Single-crystal diffraction data for **I**, **II**, and **III** were collected at 293 K with Mo K_α radiation on a Bruker SMART APEX CCD diffractometer in the form of three sets of 606 frames each with 0.3° scans in ω and exposures of 10 s per frame. The reflection intensities were integrated with the SAINT program in the SMART software package[29] over the entire reciprocal sphere. Empirical absorption corrections were completed with the aid of the SADABS program.[30] The starting atomic parameters derived via direct methods using the program SIR 97[31] were subsequently refined with the program SHELX-97[32] (full-matrix least-squares on F^2), ultimately with anisotropic atomic displacement parameters for all atoms in **I**–**IV** in the respective space groups *I*4/*mcm*, *Cmcm*, *Immm*, and *I*-4*m*2, within the WinGX program package.[33] Some details of data collection and refinement parameters are given in Table 1. The atom positional data and equivalent displacement

Table 1. Details of the Crystal Structure Investigation and Refinement for $K_{0.55(2)}Au_2Ga_2$, $KAu_{3.08}Ga_{1.92(1)}$, $KAu_{2.23}Ga_{3.77(2)}$, and $KAu_{0.33}Ga_{2.67(1)}$[a]

emp. formula	$K_{0.55(2)}Au_2Ga_2$ (**I**)	$KAu_{3.08}Ga_{1.92(1)}$ (**II**)	$KAu_{2.23}Ga_{3.77(2)}$ (**III**)	$KAu_{0.33}Ga_{2.67(1)}$ (**IV**)
formula wt	555.0	779.6	739.3	290.9
space group	*I*4/*mcm*	*Cmcm*	*Immm*	*I*-4*m*2
a, Å	8.860(3)	11.078(2)	4.4070(9)	6.0900(9)
b, Å		8.486(2)	7.339(1)	-
c, Å	4.834(2)	5.569(1)	8.664(2)	15.450(3)
volume, Å^3	379.53(2)	523.51(2)	208.22(1)	573.01(2)
Z	4	4	2	6
ρ_{calc}, g/cm^3	9.68	9.89	8.76	5.05
μ, mm^{-1}	91.403	96.382	76.282	32.268
F(000)	922	1271	602	768
θ range, deg	3.3–28.3	3.0–28.1	3.6–28.3	2.6–28.4
index ranges	$-11 \le h \le 11$	$-14 \le h \le 6$	$-5 \le h \le 5$	$-4 \le h \le 7$
	$-11 \le k \le 11$	$-11 \le k \le 10$	$-9 \le k \le 2$	$-7 \le k \le 7$
	$-6 \le l \le 6$	$-7 \le l \le 7$	$-9 \le l \le 11$	$-19 \le l \le 18$
refinement method	full-matrix least-squares on F^2			
data/restraints/parameters	146/0/14	355/0/22	210/0/16	417/0/25
goodness-of-fit on F^2	1.07	1.06	1.147	1.04
final *R* indices [$I > 2\sigma(I)$]	*R*1 = 0.015, *wR*2 = 0.035	*R*1 = 0.027, *wR*2 = 0.060	*R*1 = 0.027, *wR*2 = 0.060	*R*1 = 0.025, *wR*2 = 0.048
R_{int}	0.036	0.045	0.055	0.054
largest diff. peak and hole, e$^-$/Å^3	1.939, −1.542	2.867, −2.547	3.253, −2.078	0.652, −0.730

[a] T = 293 K; λ = 0.71073 Å.

parameters are in Table 2. The anisotropic displacement parameters of all independent atoms and additional crystallographic information (cif) are provided in the Supporting Information.

Electronic Structure Calculations. Tight binding electronic structure calculations for idealized **I**, **II**, and **III** were performed according to the linear muffin–tin–orbital (LMTO) method in the atomic sphere approximation (ASA).[34] The radii of the Wigner–Seitz spheres were assigned automatically so that the overlapping potentials would be the best possible approximations to the full potentials.[35] They were determined to be 1.53, 1.47, and 2.18 Å for Au, Ga, and K, respectively, in **I**; 1.52 and 1.64 Å for Au, 1.46 Å for Ga, and 2.12 Å for K in **II**; and 1.56 Å for Au, 1.45 Å for Ga, and 2.39 Å for K in **III**. Four empty spheres for **I** and five for **II** were needed for space filling in the atomic sphere approximation with 16% and 18% overlap restrictions between atom-centered spheres, respectively. No additional empty

dx.doi.org/10.1021/ic201999u | Inorg. Chem. 2012, 51, 1695–1702

Table 2. Atomic Coordinates and Equivalent Isotropic Displacement Parameters for I, II, III, and IV

atom	position	x	y	z	U_{eq} (Å^2)	G ≠ 1[a]
			$K_{0.55(2)}Au_2Ga_2$ (**I**)			
Ga	8h	0.38918(8)	0.11082(8)	0.5	0.0076(3)	
Au	8h	0.31672(3)	0.18328(3)	0	0.0087(2)	
K	8f	0	0	0.146(8)	0.09(3)	0.28(1)
K1	2a	0	0	0	0.033(1)	
K2	4f	0	0.5	0.8705(2)	0.032(1)	
			$KAu_{3.08}Ga_{1.92(1)}$ (**II**)			
(Au,Ga)1	8e	0.3002(2)	0.5	0	0.0089(6)	0.041/0.959(5)
Au2	8g	0.20273(6)	0.27903(7)	0.25	0.0109(2)	
Au3	4c	0	0.0727(1)	0.25	0.0112(3)	
K1	4c	0	0.6558(7)	0.25	0.019(1)	
			$KAu_{2.23}Ga_{3.77(2)}$ (**III**)			
(Au,Ga)1	8l	0	0.1969(1)	0.3526(1)	0.0119(5)	0.057/0.943(5)
Au2	4i	0	0.5	0.18120(7)	0.0125(3)	
K	2a	0	0	0	0.008(1)	
K1	2a	0	0	0	0.033(1)	
K2	4f	0	0.5	0.8705(2)	0.032(1)	
			$KAu_{0.33}Ga_{2.67}$ (**IV**)			
(Au,Ga)1	2b	0.5	0.5	0	0.0264(6)	0.214/0.786(9)
(Au,Ga)2	8i	0.7930(1)	0	0.78209(5)	0.0201(3)	0.055/0.945(6)
(Au,Ga)3	8i	0.5	0.7841(2)	0.88667(6)	0.0347(4)	0.143/0.857(7)
K1	2a	0	0	0	0.033(1)	
K2	4f	0	0.5	0.8705(2)	0.032(1)	

[a]Site occupancy.

spheres were necessary with a 16% overlap restriction for **III**. Basis sets of K 4s,4p,(3d), Au 6s,6p,5d,(4f), and Ga 4s,4p,(3d) (downfolded orbitals in parentheses) were employed. Scalar relativistic corrections were included. For bonding analysis, crystal orbital Hamilton populations (COHPs) for selected interatomic contacts were also calculated.[36]

RESULTS AND DISCUSSION

The ternary K−Au−Ga phase diagram section at 350 °C, Figure 1, has been constructed according to the exploratory synthesis and powder X-ray diffraction results. Existence of the one reported compound K_4Au_8Ga[18] was confirmed (labeled as 5 in Figure 1), and four new compounds were found. According to the existence of K_2Ga_3 and K_2Au_3, both of which contain 40 at. % K, ternary K−Au−Ga explorations were limited to <40 at. % K. No crystalline compound was found with a K content exceeding 31 at. %, namely, K_4Au_8Ga,[21] and practically every ternary compound is in equilibrium with K. A complete listing of loaded compositions and crystalline products identified by X-ray powder diffraction is in Supporting Information Table S1; the loaded compositions are marked by small, open circles on the phase diagram in Figure 1. Structural refinements for three of the four new compounds, labeled as 2 (crystal **III**), 3 (crystal **I**), and 4 (crystal **II**) in Figure 1, show essentially complete segregation of Au and Ga atoms in complex 3D networks, which in turn contain the channels for K cations. The fourth case, extracted from reaction 1 (crystal **IV**), is richest among the four examples in both K and Ga with 6−21 % Au mixed with Ga in all three network sites.

Figure 2 shows two orthogonal views each of the $K_{0.55(2)}Au_2Ga_2$ (**I**), KAu_3Ga_2 (**II**), and KAu_2Ga_4 (**III**) structures, illustrating their three-dimensional Au−Ga networks along the tunnel axes at the top and projections with the tunnels vertically oriented below. The *b* axes are horizontal in all three views. Results of the crystal structure refinements of **I**−**IV** are

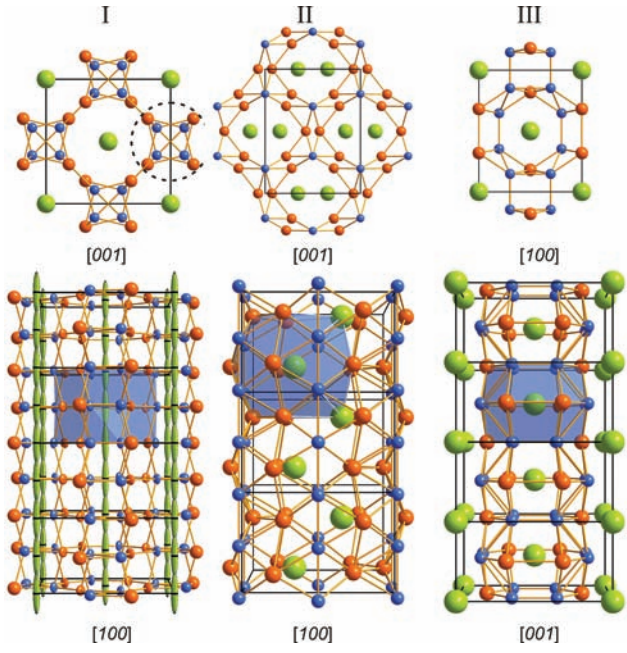

Figure 2. Crystal structures of $K_{0.55(2)}Au_2Ga_2$ (**I**), $KAu_{3.08}Ga_{1.92(1)}$ (**II**), and $KAu_{2.23}Ga_{3.77(2)}$ (**III**) with projections along and normal to cation tunnels at the top and bottom. The K, Au, and Ga atoms are light green, orange, and blue, respectively. The shaded areas in the lower views mark the cation environments.

summarized in Table 1, and atomic coordinates, equivalent isotropic displacement parameters, and occupancies of mixed Au/Ga and the K sites are listed in Table 2. Specific results for each specimen are herewith described.

$K_{0.55(2)}Au_2Ga_2$ (**I**), Figure 2 left, crystallizes in the body-centered tetragonal $K_{0.5}Pt_2Si_2$ structure type[23] with which it is also substantially isoelectronic: 8.55 valence s and p electrons/

dx.doi.org/10.1021/ic201999u | Inorg. Chem. 2012, 51, 1695−1702

f.u. for a counting scheme in which Pt and Au are assigned 0 and 1 s and p valence electrons, respectively. The Au and Ga atoms occupy the Pt and Si positions, respectively. The network structure can be described as a packing of tetrahedral stars[37] (TSs, ~stellae quadrangulae), each of which consists of an inner Ga_4 and an outer Au_4 tetrahedron, as marked in Figure 2 (top left) by a dashed circle. Each TS shares opposed rhombic faces with two others to generate a quasi-infinite rod along the *c* axis. It should be noted that there are no significant Au−Au bonds within the TSs, only Au−Ga and Ga−Ga contacts. Rather, more typical Au−Au contacts occur between the columns, 2.939(1) Å. Four such rods connect through these Au−Au and the intrarod Au−Ga bonds to form eight-membered planar and alternant Au_4Ga_4 rings. These rings stack along the *c* axis to form tunnels in which K atoms are situated in the $Au_{8/2}Ga_{8/2}$-repeating units of the tunnel. The coordination number of Au in this structure is nine, and of Ga, eight, including two K positions about each.

Potassium in this structure is not sensibly defined by anisotropic refinement of appropriate (0, 0, *z*) (8f) sites in the tunnels along *c*, which instead yields $z = 0.146(8)$, an occupancy of 0.28(1), and the extreme U_{33}/U_{11} ratio of ~36/1 for the usual centrosymmetric ellipsoid. This places the K in the general neighborhood of the Au, Ga layers but with unphysical "K−K distances" between the most probable sites of 1.01(8) and 1.41(8) Å; this reflects K disorder over a large number of tunnels, but still corresponds to one fully occupied position per tunnel per unit cell. The situation can be judged much better via the Fourier electron density computed on the basis of the observed reflections (Figure S1 in the Supporting Information). This shows a relatively large oval peak centered around $z = 0$, but with continuous lower electron densities all along *z*. (These represent the average of K positions in a very large number of channels.) For comparison, the electron density (e.d.) at the positions refined above, $z = \pm 0.146$, is 58% of $(\text{e.d.})_{max}$ at $z = 0$ with a minimum density of ~17% at $z = 0.5$.

The structure of **I** has many features similar to $K_{1.76}Au_6In_4$ and $K_{0.73}Au_2In_2$[13] in the K−Au−In system and is somewhat an average between them: the *a* axis in **I** is close to that in $K_{1.76}Au_6In_4$, but the *c* axis is similar to that in $K_{0.73}Au_2In_2$ (the difference lies only in the somewhat smaller size of Ga in comparison with In). The structural motifs in all three structures are identical: rows of TSs and eight-membered rings stacked along the *c* axis. The structure of and elemental proportions in $K_{0.73}Au_2In_2$ are very close to those in **I**: they have identical polyanionic networks and strongly disordered cation sites along the *c* axis. The only reason why $K_{0.73}Au_2In_2$ could not be refined in the higher order space group *I*4/*mcm* of $K_{0.55}Au_2Ga_2$ is the positions of electron density maxima at the K sites. In addition, the Au and In atoms alternately occupy inner and outer positions in the TS rows in the In phase.

$KAu_{3+x}Ga_{2-x}$ (**II**) (middle, Figure 2) crystallizes with an orthorhombic unit cell and is isostructural with $BaZn_5$ and $LaAl_3Ni_2$. As in **I** and other A−Au−In compounds,[13] Au and Ga build a polyanionic network that defines tunnels for the more electropositive K atoms. In contrast to both **I** and many K−Au−In compounds,[3,13,16] the tunnels here are not linear; rather, the K atoms define two-dimensional zigzag chains along the *bc* plane. This unusual packing is relatively dense and leaves no large voids in the structure.

Refinement strategies that employed segregated Ga and Au atoms among the three network sites revealed an exceptionally small isotropic displacement parameter for Ga1. Allowing Au to mix at this site improved its ellipsoidal character in comparison with other network sites and gave a statistically significant improvement in the R-factor (from 0.029 to 0.027) at the 95% confidence level according to a Hamilton test.[38] About 4% Au (an 8σ level) occupies this site, resulting in a refined composition of $KAu_{3.08}Ga_{1.92(1)}$, with a valence electron count of 9.84 *s*, *p* electrons/f.u. A small amount of Au in the Ga1 site to give a $KAu_{3+x}Ga_{2-x}$ stoichiometry is consistent with synthetic outcomes as well: reactions of 1:3:2 molar ratios of K:Au:Ga always yielded some $K_{0.5+\delta}Au_2Ga_2$ (**I**) among the crystalline products, corresponding to the need for some additional gold in the major phase.

Au−Ga and Au−Au distances lie in the ranges of 2.573(1)−2.747(1) and 2.848(1)−3.046(1) Å, respectively, and the Ga−Ga contact is 2.778(1) Å, all of which broadly correspond to the sums of covalent radii of the corresponding atoms.[39] Coordination numbers for both Au positions are 11, arising from 5-fold equatorially capped trigonal prisms, although the details of the two polyhedra differ: 4 Ga, 3 Au, and 4 K atoms around Au2, and 4 Ga, 4 Au, and 3 K atoms around Au3. Gallium atoms, with coordination number 12, form strongly distorted icosahedra and favor K neighbors somewhat.

A completely different situation exists for K, which adopts a much higher coordination number of 21, composed of 11 Au and 8 Ga (3.46−3.92 Å) in a densely packed, bowl-shaped surrounding and two additional K atoms at 3.833(8) Å. Since all K atoms are equivalent, the other two K lie at the centers of the same polyhedra, which together define the infinite 2D zigzag chains along *c* (Figure 2, bottom; Synopsis figure). A principal feature of this chain so evident in the Synopsis figure is the strong bonding of three parallel (Au2Au3) zigzag chains along each side of the K chain at 3.46−3.61 Å. Of course, the present distance does not represent a significant repulsion between K−K cations; rather, stronger K−Au and K−Ga interactions. The K positions here are fully occupied and well ordered, in contrast to that in **I**, but as mentioned above, **II** shows a small occupational disorder in the Ga site with ~4% admixed Au. The isomorphism of 10-electron **II** with the 12-electron $LaAl_3Ni_2$[24] and $BaZn_5$[25] will be briefly considered after theoretical descriptions of the electronic structure of **I** are discussed (below).

$KAu_{2+x}Ga_{4-x}$ (**III**) represents a new body-centered orthorhombic structure type, as illustrated in Figure 2 (right) along the [100] tunnel axis and in a section along the *bc* plane. The building unit of this structure is a 20-vertex K-centered $Au_{8+1.5x}Ga_{12-1.5x}$ ($x = 0.23(1)$) polyhedron with D_{2h} symmetry. This polyhedron can be described as an 8-fold equatorially capped hexagonal prism in which the hexagonal bases of the prisms ($2 \times Au_{2+x}Ga_{4-x}$) as well as the equatorial octagon ($Au_{4+x}Ga_{4-x}$) are slightly distorted. As before, the Ga site contains ~6% Au, an additional parameter that also yields a significant improvement to the overall *R* factor (from 0.031 to 0.027) at the 95% confidence level.[38] The refined composition is $KAu_{2.23}Ga_{3.77(2)}$ with a valence electron count of 14.5 valence s, p electrons/f.u.

Six such K-centered $Au_{8.68}Ga_{11.32(6)}$ polyhedra, denoted K@$Au_{8.68}Ga_{11.32(6)}$, contain K voids in the form of rhombic prisms via face- and vertex-sharing. Because all Au2 atoms are common to two such polyhedra and Ga(Au)1 sites partially belong to only one, we can formulate the phase as K@$(Au(Ga)2)_{8/2}(Ga(Au)1)_{8/2}(Ga(Au)1)_4$. The Au−Ga and Ga−Ga distances range over 2.652(1)−2.674(2) and 2.552(3)−2.937(2) Å, respectively. There is only one Au−Au contact per unit cell at a

dx.doi.org/10.1021/ic201999u | *Inorg. Chem.* 2012, 51, 1695−1702

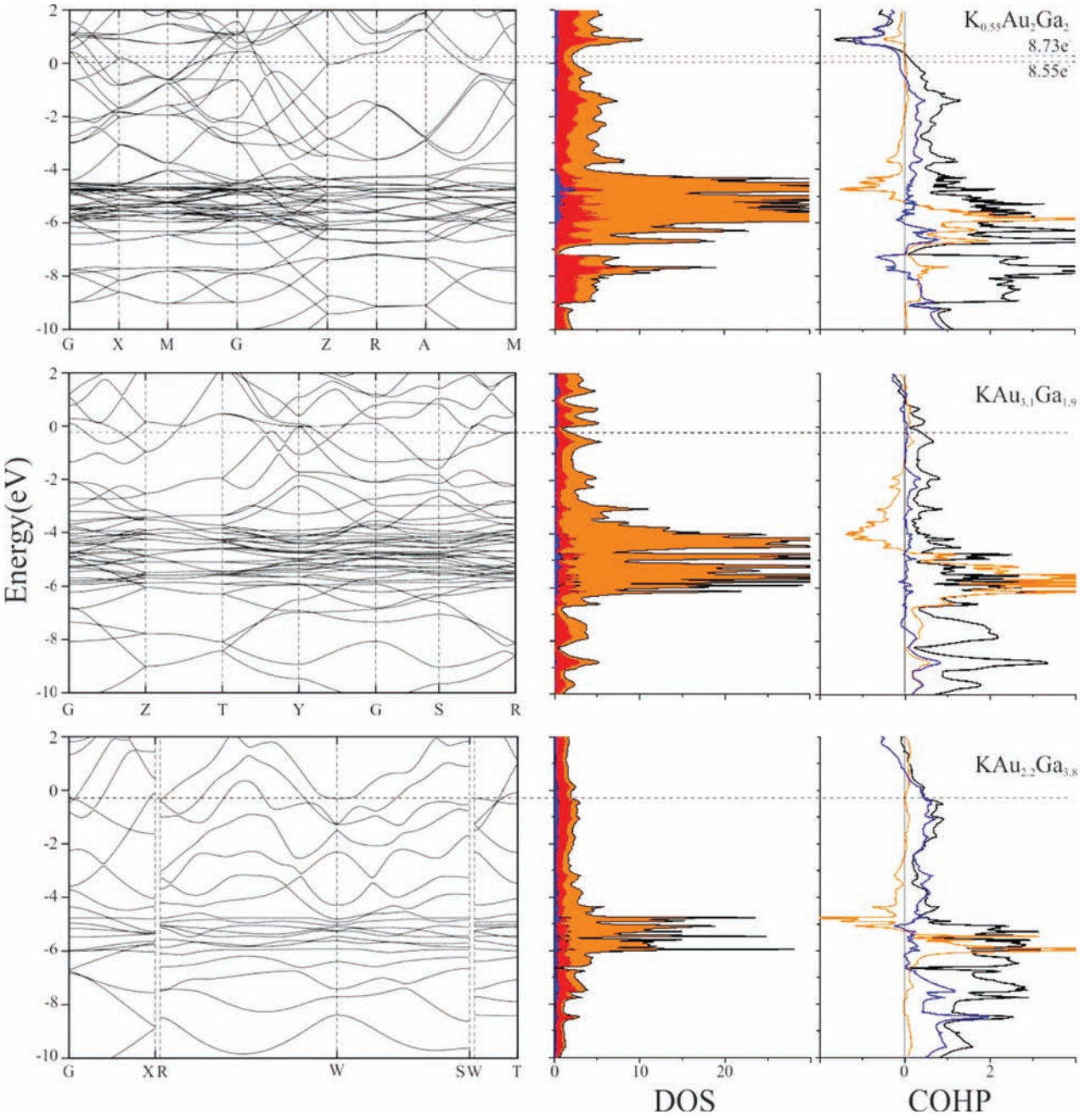

Figure 3. Results of LMTO-ASA calculations for models of **I**, **II**, and **III** (E_F dotted black line) in three parts: band structures; densities of states (total DOS (black) separated into partial DOS for gold (orange), gallium (red), and potassium (blue)); −COHP curves with Au−Ga (black), Au−Au (orange), and Ga−Ga (blue).

distance of 3.141(2) Å, somewhat longer than those in comparable indides.[3,6,10−16] In contrast to **I** and **II**, the K atoms in **III** are well ordered and separated, with a K···K distance of 4.407 Å. In terms of tunnels, the present compound can be presented as an average variant of **I** and **II**: the tunnels are linear as in **I**, but with cations surrounded by Au/Ga cages, as observed in **II**. It also compares well with two indides, KAu_4In_6 and $SrAu_3In_3$, both of which contain similar $M@(Au,In)_{21}$ single building units. The latter can also be described in terms of rather ideal hexagonal prisms ($2 \times Au_3In_3$) that are, however, 9-fold (Au_3In_6) equatorially capped.

$KAu_{0.33}Ga_{2.67}$ (**IV**) crystallizes with a tetragonal unit cell and is isostructural with KGa_3[40] and $RbAu_xGa_{3-x}$.[41] A continuous series of compounds with composition KAu_xGa_{3-x}, $0 \le x \le 0.33$, can be synthesized with **IV** as the saturation point at room temperature. Since the building principles have been described in detail before,[35] only general comments and comparisons will be provided here. The main structural features are $(Ga,Au)_8$ dodecahedral clusters with ~6, 14, or 21% Au mixed in all three Ga positions. These clusters are linked via either direct intercluster bonds or additional bridging (Ga,Au) sites along *c* to create a layered polyanionic network in which K cations lie (Figure S2, Supporting Information). Coordination numbers of the cluster atoms are 5 and 6, which correspond to somewhat distorted tetragonal and pentagonal pyramids, and the bridging atoms are tetrahedral. Linear chains of K atoms lie along the *a*/*b* axes, similar to those in **I** and **III**, plus zigzag chains of K atoms along *c*, similar to that in **II** along *c*. Substituting Au into

dx.doi.org/10.1021/ic201999u | *Inorg. Chem.* 2012, 51, 1695−1702

the structure of KGa_3 decreases the *a* parameter from 6.268 to 6.090 Å (3%) at saturation, but increases *c* from 14.782 to 15.450 Å (4%), resulting in an ~1% increase in the unit cell volume. Despite somewhat different radii of Au and Ga, such changes cannot be explained directly by substitution of Ga by Au because of different (6−21% Au) distributions in the three Ga sites. These variations are caused mainly by changes in intracluster distances Ga2−Ga3 (2.60 and 2.65 Å in KGa_3 and **IV**, respectively), which lead to cluster distortions, whereas intercluster distances more or less along *c* change insignificantly with additional Au. All of these changes are comparable to those found between $RbGa_3$ and $RbAu_xGa_{3-x}$.[41]

Electronic Structures and Chemical Bonding. The electronic densities of states (DOS) curves for idealized **I** (KAu_4Ga_4), **II** (KAu_3Ga_2), and **III** (KAu_2Ga_4) in Figure 3 are all qualitatively similar, with broad valence s,p bands extending ~10 eV below the Fermi levels (E_F) and a large, mostly Au 5d band located 4−6 eV below E_F. The position of the Au 5d band allows the assignment of formally filled 5d orbitals to gold in valence electron counting approaches, although there is little doubt that the mixing of these with higher lying valence orbitals is important in its bonding. The similarities in these electronic structure results stem from their structural parallels; there are significantly more heteroatomic Au−Ga contacts in the formally anionic networks than homoatomic Au−Au or Ga−Ga bonds. All Fermi levels, which have been adjusted to match the refined chemical compositions of each case, intersect low, nonzero DOS regions, indicating poor metallic characteristics. In all three cases, the shift in the Fermi level from that of the idealized compositions lowers the DOS values, which is specifically achieved by adding valence electrons to "KAu_4Ga_4" (**I**), but by removing electrons from "KAu_3Ga_2" (**II**) and "KAu_2Ga_4" (**III**). Furthermore, the features near the Fermi levels in the DOS curves for cases **I** and **II** resemble pseudogaps, which are emphasized by the band structures also illustrated in Figure 3. A distinct pseudogap is not seen for **III**.

Decompositions of the DOS curves into their atomic orbital components reveal that valence orbitals of K contribute rather little to the occupied states, with some minor enhancements among the Au 5d bands. This outcome identifies K as formally K^+ in all cases. The relativistic effects on Au 6s states are evident as they contribute significantly along with Ga 4s states below the large Au 5d bands, which are slightly different in the three cases. In particular, the Au 5d bandwidth decreases along the sequence "KAu_3Ga_2" (**II**), "KAu_4Ga_4" (**I**), "KAu_2Ga_4" (**III**), in line with the decreasing Au proportions. There are simply fewer Au−Au nearest-neighbor contacts along the series. Furthermore, the contributions of the two distinctive Au positions in **II** are somewhat different: within the same broad band, Au2 orbitals contribute more at higher energies, ~−3.5 eV, whereas Au3 orbitals are more significant around ~−4.5 eV. This outcome emerges from the different environments: Au2 is surrounded by seven electronegative metals and four K atoms; Au3 is coordinated by eight electronegative metals and three K atoms.

Adding valence electrons to "KAu_4Ga_4" (**I**) both lowers the DOS at the Fermi level, as mentioned above, and increases the heteroatomic Au−Ga bonding overlap, as seen in the COHP curve in Figure 3. However, Ga−Ga antibonding interactions also increase. Thus, this structure introduces additional valence electron density by increasing the K content by 10% to $K_{1.10}Au_4Ga_4$ rather than by substituting Ga at Au sites, that is, via "$KAu_{4-\delta}Ga_{4+\delta}$". Optimization of heteroatomic Au−Ga interactions occurs at "$K_{1.5}Au_4Ga_4$" with a valence electron count of 17.46 electrons/f.u. With this outcome in mind, total energy calculations were performed for **I** with different positions for K atoms along the *c* axis (z = 0, 0.1, 0.2, 0.25, 0.3, 0.4). The Wigner−Seitz radii of the three atomic positions were fixed at the values used for K at z = 0 (1.53, 1.47, and 2.18 Å for Au, Ga, and K, respectively). Relative minima showing most probable positions of K atoms occurred at z = 0 and 0.25. The global minimum is at z = 0.25, which places K atoms at the midpoints between adjacent planes of Au and Ga nets. The total energies when K atoms occupy positions z = 0.2 and 0.3 were found to be 0.36−0.42 eV higher than that of z = 0.25 (Figure S4 in Supporting Information). Thus, there is energetic frustration between optimizing K−Au and K−Ga vs K···K interactions.

In **II** and **III**, lowering of the valence electron counts moves the Fermi levels toward local minima in the DOS curves. As seen in refinements of single crystal X-ray diffraction data, these changes occur by replacing some Ga atoms with Au. Unlike **I**, however, this change in valence electron count removes electrons from bonding orbital interactions within the polyanionic frameworks, so the observed valence electron counts in both **II** and **III** seem to be driven by achieving lower DOS values at their Fermi levels. One final point: in the band structure calculations for **II**, we observe characteristic flat bands along the Brillouin zone line Z−T, T−Y, and Y−G, which are crossed by broad bands, features that can indicate possible superconductivity;[42] however, preliminary magnetic measurements on powder samples of **II** at 2−300 K did not show any effects (Figures S5 and S6 of the Supporting Information).

To compare interatomic orbital interactions in **I**, **II**, and **III**, crystal orbital Hamilton population analyses have been performed (see −COHP curves in Figure 3). The weighted and integrated crystal orbital Hamilton population (−ICOHP) values for near-neighbor contacts are summarized in Table 3. In each compound, the greatest contributions to the total orbital interactions arise from Au−Ga contacts, providing 55−72% of the total bonding population. As for **I**, a larger population appears for Au−Ga contacts forming the tunnels around K, and both Au−Ga and Ga−Ga populations give more than 80% of the total, whereas K−Au and K−Ga contributions to the total appear to be insignificant. As mentioned above and seen in the −COHP curves in Figure 3, Au−Ga, Au−Au, and Ga−Ga orbital interactions in **I** are nearly optimized at E_F, and a larger number of valence electrons would populate Ga−Ga antibonding states. Electronic structure calculations were also performed for isostructural and isoelectronic compound $K_{0.5}Pt_2Si_2$. The bonding analysis for $K_{0.5}Pt_2Si_2$ (Table 3), is quite similar to the outcome for $K_{0.55}Au_2Ga_2$. Since the covalent radii of Au and Pt are very similar, the unit cell volume reduction is caused mainly by Si, which results in unit cell parameters 6% smaller than the gallide.

Somewhat different situations are observed in **II** and **III**. Au−Ga bonding plays the dominant role in both cases (60−70% of the total); as in **I**, the contributions of homoatomic Au−Au or Ga−Ga interactions depend on the frequency of contacts in each structure. In **II**, there are three different Au−Ga bond distances (2.573, 2.686, and 2.747 Å), two different Au−Au separations (2.848 and 3.015 Å), and only one Ga−Ga contact (2.784 Å). Both homoatomic Au−Au and Ga−Ga interactions are optimized at E_F, whereas the Au−Ga interaction remains bonding until ~1 eV higher. Thus, although

dx.doi.org/10.1021/ic201999u | Inorg. Chem. 2012, 51, 1695−1702

Table 3. Bond Length Ranges and Average −ICOHP Values in I−III and $K_{0.5}Pt_2Si_2$.[20]

bond type	length (Å)	−ICOHP (eV/per av bond)	no./cell	−ICOHP (eV/cell)	contribution (%)
		"$K_{0.5}Au_2Ga_2$" (model for **I**)			
Au−Ga	2.582−2.684	1.637	48	78.58	85.7
Au−Au	2.939	0.970	8	7.76	8.5
Ga−Ga	2.777−3.114	0.507	8	4.05	4.4
K−Au	3.318	0.075	12	0.9	1
K−Ga	3.654	0.036	12	0.43	0.5
		$K_{0.5}Pt_2Si_2$			
Pt−Si	2.40−2.48	2.342	48	112.41	87.6
Pt−Pt	2.782	1.285	8	10.28	8
Si−Si	2.624−2.946	0.602	8	4.82	3.8
K−Pt	3.389	0.039	12	0.47	0.4
K−Si	3.823	0.028	12	0.34	0.3
		"KAu_3Ga_2" (model for **II**)			
Au−Ga	2.571−2.747	1.178	48	56.54	72.2
Au−Au	2.848−3.013	0.787	20	15.74	20.1
Ga−Ga	2.784	0.545	8	4.36	5.6
K−Au	3.454−3.904	0.03	44	1.32	1.7
K−Ga	3.850−3.921	0.01	32	0.32	0.4
		"KAu_2Ga_4" (model for **III**)			
Au−Ga	2.652−2.674	1.882	24	45.17	71.3
Au−Au	3.141	1.036	1	1.04	1.6
Ga−Ga	2.552−2.937	1.198	12	14.38	22.7
K−Au	3.533−3.991	0.05	8	0.4	0.6
K−Ga	3.380−3.381	0.10	24	2.4	3.8

homoatomic bonding does not provide the major energetic stability for this structure, it does influence the valence electron count. In **III**, homoatomic Au−Au interactions seem to control the valence electron count because these orbital overlaps are optimized at the Fermi level, whereas Au−Ga and Ga−Ga contacts have unoccupied bonding states above E_F.

The existence of 12-electron $LaAl_3Ni_2$[24] and $BaZn_5$,[25] which are isomorphous to **II**, raises some interesting and complex questions about bonding distributions, particularly for the latter, in which zinc atoms are distributed over the three independent Ga (8e) and Au (8 g and 4c) sites in 10-electron KAu_3Ga_2. The distances in these two phases are compared in Table 4 according to bond types. Equivalence is not expected,

Table 4. Comparison of Distance Distributions between Equivalent Atom Pairs in Isomorphous $BaZn_5$ and "KAu_3Ga_2"

$BaZn_5$	Å	KAu_3Ga_2	Å
Zn1−Zn2	2.59	Au2−(Au,Ga)1	2.57
Zn3−Zn1	2.65	Au3−(Au,Ga)1	2.68
Zn1−Zn1	2.66	(Au,Ga)1−(Au,Ga)1	2.78
Zn3−Zn2	2.66	Au2−Au3	2.85
Zn1−Zn2	2.67	Au2− (Au,Ga)1	2.75
Zn3−Zn3	2.94	Au3−Au3	3.04
Zn2−Zn2	2.98	Au2−Au2	3.01

but parallels perhaps. The foregoing Hamilton population data for the ternary phase emphasize the greater role that polar Au−Ga contributions make, and this seems consistent among the first four distance entries, but the last three of both kinds are somewhat longer in KAu_3Ga_2. Aluminum in the parallel $LaAl_3Ni_2$ takes the 8g (and 4c) site, parallel to Au2, leaving the more electronegative Ni in the Ga equivalent with more La neighbors, somewhat of a contrary situation. Nonetheless, the intrinsic electronic stability of this structure type for 12 valence electrons/f.u. is evident from the DOS and −COHP curves of KAu_3Ga_2: there is a clear pseudogap in the DOS for 12 valence electrons (~1 eV above E_F in Figure 3), and the Au−Ga interactions are optimized at this band filling. A DOS curve calculated for $BaZn_5$ does not indicate similar definitive pseudogaps near 10- and 12-electron cases.

Orbital interactions in the polyanionic network also influence the maximum level of Au substitution into KGa_3. Compound **IV**, $KAu_{0.33}Ga_{2.67}$, has 0.67 fewer valence electrons than 10-electron KGa_3. According to previously reported extended Hückel calculations,[41] the DOS of KGa_3 shows an energy gap at its Fermi level, but these calculations neglected inclusion of K atoms, which have very diffuse valence orbitals and are not treated well by this semiempirical method. A DOS curve of KGa_3 calculated by the TB-LMTO-ASA approach (presented as Figure S7 in the Supporting Information) also gives an energy gap for 10 valence electrons per formula unit, but reveals a modest pseudogap for 9.33 electrons/f.u. Lowering the Fermi level by further substitution of Au for Ga would deplete valence electrons from the large peak in the DOS curve, states which are strongly Ga−Ga bonding in KGa_3.[41]

Physical Properties. Magnetic susceptibility measurements were carried out between 2 and 350 K with the aid of a Quantum Design (MPMS) SQUID magnetometer. Polycrystalline samples, 92.4 mg of **I** and 30.2 mg of **II**, were held in fused silica capillaries. The temperature dependence of the magnetic susceptibility for both compounds is shown in the Supporting Information (Figures S5 and S6). The susceptibility of **II** is rather small, positive, and almost temperature-independent, with a value of $\chi_m \approx 2.6 \times 10^{-3}$ emu·mol^{-1} at 0.1 T over the range of 100−300 K, suggesting that the compound is essentially Pauli paramagnetic, consistent with the expected metallic character. The magnetic susceptibility of **I** is also temperature-independent over the range of 70−300 K, similar in magnitude, but negative: $\chi_m \approx -3.9 \times 10^{-3}$ emu·mol^{-1} at 1 T and $\chi_m \approx -4.1 \times 10^{-3}$ emu·mol^{-1} at 2 T. In all three cases, we can see an increase in the susceptibility below 100 K, an observation that can only be explained by magnetic impurities that are not detectable by powder diffraction.

SUMMARY

The K−Au−Ga system has been investigated systematically and four new ternary compounds have been discovered. $KAu_{2+x}Ga_{4-x}$ crystallizes with a new structure type, and $K_{0.55}Au_2Ga_2$, $KAu_{3+x}Ga_{2-x}$, and $KAu_{0.33}Ga_{2.67}$ are isostructural with known phases, respectively, KPt_2Si_2, $BaZn_5$, and $RbAu_xGa_{3-x}$. $K_{0.55}Au_2Ga_2$ is also isoelectronic with KPt_2Si_2. Analysis of electronic structure calculations reveals that the compounds are metallic in nature. Furthermore, the overall bond populations are dominated by polar Au−Ga bonds, whereas the observed valence electron counts are influenced by homoatomic Au−Au and Ga−Ga interactions, which lead to nonstoichiometric compositions in each.

ASSOCIATED CONTENT

Supporting Information

cif outputs for four structures; analysis of loaded K−Au−Ga compositions; anisotropic displacement parameters; illustration of KAu_xGa_{3-x} (**IV**); Fourier map of K in **II**; DOS and COHP

dx.doi.org/10.1021/ic201999u | Inorg. Chem. 2012, 51, 1695−1702

curves for **I**–**III** magnified near E_F; relative total energies of different "KAu_4Ga_4" motifs; magnetic susceptibilities for **I** and **II**; and DOS curve for KGa_3. This material is available free of charge via the Internet at http://pubs.acs.org

AUTHOR INFORMATION

Corresponding Author

*E-mail: gmiller@iastate.edu (G.J.M.), jcorbett@iastate.edu (J.D.C.).

ACKNOWLEDGMENTS

We are indebted to Y. Mudryk, Ames Laboratory, for the magnetic susceptibility data. We also wish to thank an astute reviewer for numerous helpful comments. The research was supported by the Office of the Basic Energy Sciences, Materials Sciences Division, U.S. Department of Energy (DOE). Ames Laboratory is operated for DOE by Iowa State University under contract No. DE-AC02-07CH11358.

REFERENCES

(1) Corbett, J. D. In *Chemistry, Structure and Bonding of Zintl Phases and Ions*; Kauzlarich, S., Ed.; VCH Publishers: New York, 1996, Chapter 3.
(2) Corbett, J. D. *Angew. Chem., Int. Ed.* **2000**, *39*, 670.
(3) Li, B.; Kim, S.-J.; Miller, G. J.; Corbett, J. D. *Inorg. Chem.* **2009**, *48*, 6573.
(4) Zachwieja, U. *Z. Anorg. Allg. Chem.* **1997**, *623*, 1621.
(5) Henning, R. W.; Corbett, J. D. *Inorg. Chem.* **1999**, *38*, 3883.
(6) Li, B.; Corbett, J. D. *Inorg. Chem.* **2005**, *44*, 6515.
(7) Li, B.; Corbett, J. D. *Inorg. Chem.* **2004**, *43*, 3582.
(8) Tillard-Charbonnel, M.; Belin, C. *Mater. Res. Bull.* **1992**, *27*, 1277.
(9) Tillard-Charbonnel, M.; Chahine, A.; Belin, C. *Z. Kristallogr.* **1993**, *208*, 372.
(10) Li, B.; Corbett, J. D. *Inorg. Chem.* **2006**, *45*, 8958.
(11) Li, B.; Corbett, J. D. *J. Am. Chem. Soc.* **2005**, *127*, 926.
(12) Pearson, R. G. *Inorg. Chem.* **1988**, *27*, 734.
(13) Li, B.; Corbett, J, D. *Inorg. Chem.* **2007**, *46*, 6022.
(14) Samal, S. L.; Corbett, J. D. *Inorg. Chem.* **2011**, *50*, 7033.
(15) Chai, P.; Corbett, J. D. *Inorg. Chem.* **2011**, *50*, 10949.
(16) Li, B.; Corbett, J. D. *J. Am. Chem. Soc.* **2006**, *128*, 12392.
(17) Zachwieja, U. *J. Alloys Comp.* **1996**, *235*, 7.
(18) Zachwieja, U. *Z. Anorg. Allg. Chem.* **1996**, *622*, 1581.
(19) Zachwieja, U. *Z. Anorg. Allg. Chem.* **1995**, *621*, 1677.
(20) Tillard-Charbonnel, M.; Belin, C. *Z. Kristallogr.* **1993**, *206*, 310.
(21) Mueller, J.; Zachwieja, U. *Z. Anorg. Allg. Chem.* **2000**, *626*, 1867.
(22) Henning, R. W.; Corbett, J. D. *J. Alloys Compd.* **2002**, *338*, 4.
(23) Thronberens, W.; Sinnen, H. D.; Schuster, H. U. *J. Less-Common Met.* **1980**, *76*, 99.
(24) Gladyshevskii, R. E.; Cenzual, K.; Parthé, E. *Acta Crystallogr.* **1992**, *B48*, 389.
(25) Baenziger, N. C.; Conant, J. W. *Acta Crystallogr.* **1956**, *9*, 361.
(26) Wendorff, M.; Röhr, C. *Z. Naturforsch.* **2007**, *B62*, 1549.
(27) Dong, Z.-C.; Corbett, J. D. *J. Am. Chem. Soc.* **1993**, *115*, 11299.
(28) *WinXPow 2.10*; Stoe & Cie GmbH: Darmstadt, Germany, 2004.
(29) *SMART*; Bruker AXS, Inc.; Madison, WI, 1996.
(30) Blessing, R. H. *Acta Crystallogr.* **1995**, *A51*, 33.
(31) Altomare, A.; Burla, M.; Camalli, M.; Carroccini, B.; Cascarano, G.; Giacovazzo, C.; Guagliardi, A.; Moliterni, A.; Polidori, G.; Rizzi, R. *J. Appl. Crystallogr.* **1999**, *32*, 115.
(32) Sheldrick, G. M. *SHELXL-97: Program for the Refinement of Crystal Structures*, University of Göttingen, Germany, 1997.
(33) Farrugia, L. *J. Appl. Crystallogr.* **1999**, *32*, 837.
(34) Krier, G.; Jepsen, O.; Burkhardt, A.; Andersen, O. K. *TB-LMTO-ASA Program, version 4.7*; Max-Planck-Institut für Festkörperforschung: Stuttgart, Germany, 1995.
(35) Jepsen, O.; Andersen, O. K. *Z. Phys. B* **1995**, *97*, 35.
(36) Dronskowski, R.; Blöchl, P. E. *J. Phys. Chem.* **1993**, *97*, 8617.
(37) Schubert, K., *Kristallstrukturen zweikomponentiger Phasen*, Springer, Berlin, 1964, p 150.
(38) Hamilton, W. C. *Acta Crystallogr.* **1965**, *18*, 502.
(39) Cordero, B.; Gomez, V.; Platero-Pratz, A.; Reves, M.; Echeverría, J.; Cremades, E.; Barragán, F.; Alvarez, S. *Dalton Trans.* **2008**, *2008*, 2832.
(40) Ling, R.; Belin, C. *Z. Anorg. Allg. Chem.* **1981**, *480*, 181.
(41) Henning, R. W.; Corbett, J. D. *J. Alloys Compd.* **2001**, *338*, 4.
(42) Deng, S.; Simon, A.; Köhler, J. *Solid State Sci.* **2000**, *2*, 31.